

# Control of Molecular and Microdomain Orientation in a Semicrystalline Block Copolymer Thin Film by Epitaxy

Claudio De Rosa,<sup>†,‡</sup> Cheolmin Park,<sup>§</sup> Bernard Lotz,<sup>‡</sup> Jean-Claude Wittmann,<sup>‡</sup> Lewis J. Fetters,<sup>§</sup> and Edwin L. Thomas<sup>\*,†</sup>

Department of Materials Science and Engineering, Massachusetts Institute of Technology, Cambridge, Massachusetts 02139, Institut Charles Sadron, CNRS, 6 rue Boussingault, 67083 Strasbourg, France, and Exxon Mobil Research and Engineering Company, Corporate Strategic Research, Annandale, New Jersey 08801

Received December 21, 1999; Revised Manuscript Received April 5, 2000

**ABSTRACT:** Epitaxial crystallization is utilized to control both molecular chain orientation and microdomain structure in a thin film of a semicrystalline triblock copolymer, composed of crystallizable polyethylene (PE) end blocks and an amorphous ethylene-*alt*-propylene (PEP) midblock where the microphase separation is driven by crystallization from a homogeneous melt, characterized by small-angle and wide-angle X-ray diffraction. Surface interaction due to a crystallographic matching of unit cells between the crystalline PE block and benzoic acid (BA) substrate induces high orientation of the crystalline PE block, resulting in a well-ordered parallel lamellar microphase-separated structure. The excellent orientation induced by the surface interaction is evidenced by the selected area electron diffraction (SAD) pattern and bright-field (phase contrast) and dark-field (diffraction contrast) transmission electron microscope (TEM) images of the block copolymer thin film. The data clearly show that the chain axis ( $\hat{c}$ ) of PE is parallel to the normal ( $\hat{n}$ ) of the microphase-separated lamellar surfaces.

## Introduction

The driving force for microphase separation in amorphous block copolymers is the incompatibility between the blocks that are chemically linked.<sup>1</sup> The resulting ordered microstructures have periods on the order of the polymer chain dimensions; different microphase-separated morphologies can form depending on the inherent block incompatibility (characterized by  $\chi$ , the Flory–Huggins segmental interaction parameter, which is generally found to be inversely proportional to the temperature), the total degree of polymerization ( $N_t$ ), and the volume fraction of the components.<sup>2</sup> For high values of the product  $\chi N_t^{2-4}$  the block copolymer is strongly segregated, and well-organized microdomain structures result. For low values of the product  $\chi N_t$  (low block incompatibility and/or low molecular weight and/or at high temperature) the block copolymer presents a homogeneous disordered phase.

In block copolymers which contain one or more crystallizable blocks, microphase separation can result either from incompatibility of the blocks or by crystallization of some block. The final morphology will be the result of the interplay between microphase separation of the component blocks and the crystallization of the crystallizable blocks.

Early work by Skoulios et al.<sup>5</sup> and Lotz et al.<sup>6,7</sup> on semicrystalline block copolymers was concerned with the influence of an attached amorphous block on the nature of the chain folding of the crystalline block in poly(styrene-*b*-ethylene oxide). More recently, various groups<sup>8–33</sup> have shown that the morphology of semi-

crystalline block copolymers is path-dependent; different microdomain structures are obtained if the crystallization occurs from a homogeneous melt (in this case the crystallization drives the microphase separation), or it occurs from an already microphase-separated heterogeneous melt. (In this case microphase separation precedes crystallization and provides a microstructure within which crystallization takes place.)

When the block incompatibility is small, as for instance for the block copolymers composed of crystallizable polyethylene (PE) blocks and poly(ethylene-*alt*-propylene) (PEP) or poly(ethylene) amorphous blocks, such as those analyzed by Rangarajan et al.,<sup>13,16</sup> crystallization occurs from a homogeneous melt resulting in the formation of alternating lamellar microdomains in a spherulitic superstructure regardless of the copolymer composition,<sup>13</sup> as has been assumed in theoretical treatments.<sup>34,35</sup>

When the segments are highly incompatible and also have large molecular weights, microphase separation in the melt occurs prior to crystallization. The presence of microdomains in the ordered melt may affect the crystallization process and the final morphology.<sup>8,9,12,20,26–28,32,33</sup>

The orientation of the chain axis ( $\hat{c}$ ) within crystalline lamellae in the confined superstructure has also been widely studied.<sup>11,13–16,21,26,28,29,32,33</sup> The relationship between  $\hat{c}$  and the normal direction ( $\hat{n}$ ) of microphase-separated lamellar surfaces turned out to be very complex, influenced by many factors such as molecular weight of the block copolymer and crystallization temperature of the crystalline block and so on. A model in which  $\hat{c}$  is oriented *parallel* to  $\hat{n}$  of microphase-separated lamellar surfaces has been proposed on the basis of experimental observations on PE containing block copolymers,<sup>13,16</sup> for which the polymer is crystallizing from a homogeneous melt or within a weakly microphase-segregated state. On the other hand, other experimental

<sup>†</sup> Massachusetts Institute of Technology.

<sup>‡</sup> Institut Charles Sadron.

<sup>§</sup> Exxon Research and Engineering Company.

\* To whom correspondence should be addressed. Tel 617-253-6901; FAX 617-258-6135; e-mail elt@mit.edu.

<sup>‡</sup> Present address: Dipartimento di Chimica, Università di Napoli "Federico II", Via Mezzocannone 4, 80134 Napoli, Italy.

observations have indicated that crystallization from an ordered microphase-separated melt results in  $\hat{c}$  aligned perpendicular to  $\hat{n}$  of the lamellar microdomain surfaces.<sup>11,14,15,21,33</sup>

An important parameter that influences the orientation of the chains with respect to the domain interface in lamellar systems seems to be the molecular weight.<sup>21,29</sup> Ryan et al.<sup>19,23</sup> have shown that the number of folds in the low molecular weight regime is coupled to the conformational state of the amorphous block. The metastable structures developed during various heat treatments show different folding behavior of the semicrystalline block. In addition, the equilibrium conformation of the semicrystalline block depends on the molecular weights of both the semicrystalline and amorphous blocks.<sup>24</sup> As the total molecular weight increases, the interfacial area per junction is increased, and the crystalline stems tilt and eventually become parallel to the lamellar interface to match the preferred interfacial area of the amorphous chain.<sup>21,29</sup> Recently, Zhu et al. showed that the variation of the crystallization temperature of the crystalline block depends different orientations ( $\hat{c} \perp \hat{n}$  at low  $T_c$ , inclined at intermediate  $T_c$ , and  $\hat{c} \parallel \hat{n}$  at the highest  $T_c$ ) of the crystals with respect to the microphase-separated structure at fixed molecular weight.<sup>33</sup>

It is worth noting that in many of the cited papers the determination of the orientation of the chains in the crystalline domains has been achieved by employing methods that are normally used to induce alignment of the microdomains, that is, by application of an external bias field, such as thermomechanical plane strain compression (channel die)<sup>14,15,26,28</sup> or oscillatory shear.<sup>11,21</sup> These methods achieve good alignment of the microdomains; however, the resulting orientation of the molecular chains in the crystalline phase, usually detected by wide-angle X-ray diffraction, is often very low, making detailed modeling of the crystalline structure and microdomain structure problematic and raising the issue of the role of the applied field on the boundary conditions so formed. In addition, these processing methods are hardly applicable for patterning thin films.

The epitaxial crystallization of PE homopolymer on various substrates has been extensively studied; inorganic substrates (e.g., alkali halides),<sup>36</sup> polymer substrates (e.g., oriented films of poly(tetrafluoroethylene)),<sup>37</sup> and organic substrates (e.g., benzoic acid, condensed aromatic hydrocarbons, and linear polyphenyls)<sup>38,39</sup> have been successfully used to grow well-oriented crystals of PE. Although the versatility of these substrates has been clearly shown, attempts of using them to control the crystallization and its orientation as well as to investigate the resulting morphology of the thin film of semicrystalline block copolymers is new.

In this paper the PE blocks in a semicrystalline triblock copolymer are epitaxially crystallized onto the surface of crystals of benzoic acid (BA). Our goal is to obtain a high orientation of the crystals in a semicrystalline triblock copolymer thin film. The triblock has PE as crystallizable end blocks and a noncrystalline rubbery midblock composed of alternating ethylene and propylene units. The external field generated by the crystallographic matching of PE crystal and BA crystal provides a way to control not only the molecular chain orientation of PE block but also the resulting microphase-separated structure. In addition, the high orientation of the suprastructure allows precise deter-

mination of the angle between  $\hat{c}$  and  $\hat{n}$  by employing SAD, bright field (BF) TEM, and dark field (DF) TEM.

## Experimental Procedures

The poly(ethylene-*b*-(ethylene-*alt*-propylene)-*b*-ethylene) triblock copolymer (PE/PEP/PE) was prepared by catalytic hydrogenation of poly(1,4-butadiene-*b*-1,4-isoprene-*b*-1,4-butadiene) (PB/PI/PB). The latter was synthesized by anionic polymerization in benzene at 20 °C with *sec*-butyllithium as initiator according to the standard high-vacuum techniques.<sup>40</sup> The 1,4-additions of butadiene and isoprene units in the PB/PI/PB block copolymer give rise, after hydrogenation, to the PE end blocks and the alternating copolymer of ethylene and propylene (PEP) in the PE/PEP/PE copolymer. The small percentage of 3,4-additions of isoprene units produces, after hydrogenation, isopropyl branches in the PEP block, while the small percentage of 1,2-additions of butadiene units produces ethyl branches in the PE blocks. The estimated number of ethyl branches per 100 backbone carbon atoms in the PE block is two.<sup>41</sup> The hydrogenation reaction was carried out using the standard procedure described elsewhere.<sup>41</sup> The solvent was heptane, and the catalyst was palladium on calcium carbonate. <sup>1</sup>H NMR showed that no double bonds remained.

Molecular weight characterizations were done using a combination of size exclusion chromatography (SEC) and low-angle laser light scattering. Tetrahydrofuran was used as solvent in both cases. For the PB/PI/PB sample the average molecular weight via light scattering was  $M_w = 55\,000$  g/mol, while SEC gave  $M_z/M_w$  and  $M_w/M_n$  ratios of 1.02 and 1.03, respectively. The molecular weight of each poly(1,4-butadiene) end block was approximately 10 000 g/mol, while that of the polyisoprene midblock was approximately 35 000 g/mol. Essentially the same molecular weights result for the corresponding hydrogenated blocks in the PE/PEP/PE sample. From the weight fractions of the blocks and assuming for the PE and PEP blocks densities at 140 °C of 0.78 and 0.79 g/cm<sup>3</sup>,<sup>42</sup> respectively, a volume fraction of the PE blocks in the block copolymer melt of 0.37 was estimated.

The melting temperature and the crystallinity index of the bulk polymer were obtained with calorimetric measurements using a Perkin-Elmer DSC-7, performing scans in a flowing N<sub>2</sub> atmosphere at heating rate of 2 °C/min. The crystallinity index was calculated from the values of the experimental melting enthalpy and the value of the equilibrium melting enthalpy of a perfect crystal of PE (289 J/g).<sup>43</sup> The crystallinity index of a sample crystallized from the melt by cooling to room temperature at a cooling rate of 2 °C/min was nearly 30% with respect to the crystallizable PE blocks, corresponding to only about 10% with respect to the total weight of the block copolymer sample. The melting temperature of the PE/PEP/PE sample was 102 °C, significantly lower than that of a high-density PE, indicative of the presence of the ethyl branches.

The bulk samples of the block copolymer used in the small-angle (SAXS) and wide-angle (WAXS) X-ray diffraction experiments were prepared by melting and recrystallization in order to eliminate any previous thermal history.

In-situ SAXS and WAXS measurements were carried out at the Advanced Polymer beamline, X27C, National Synchrotron Light Source (NSLS), Brookhaven National Laboratory (BNL). The wavelength used was  $\lambda = 0.1307$  nm, and the beam size at the sample position was about 0.4 mm in diameter. A three 2° tapered tantalum pinhole collimation system was used with sample-to-detector distances of 1560 and 108 mm for the SAXS and WAXS patterns, respectively. Scattering angles  $2\theta$  down to 1.5 mrad, corresponding to a spacing ( $d = 2\pi/q$ , where  $q = 4\pi \sin \theta/\lambda$ ) of about 100 nm, were achieved in the SAXS pattern. The SAXS and WAXS patterns were recorded at various temperatures using a single-cell heating stage (maximum temperature: 350 °C). The sample was melted, and the patterns were recorded at different temperatures starting from the melt and cooling to room temperature at a cooling rate of 2 °C/min. Fuji imaging plates were used to collect the scattering data with exposure times of 1 min per frame. The isotropic diffraction data were circularly averaged over the

azimuthal coordinate of the two-dimensional patterns and plotted as a function of the scattering vector  $q$  and the Bragg angle  $2\theta$  for the SAXS and WAXS pattern, respectively.

Epitaxial crystallization of the block copolymer onto BA was performed following the procedure developed for the PE homopolymer.<sup>38</sup> Thin films of the block copolymer were first formed on carbon-coated microscope glass slides by casting from xylene solution (0.1–0.3 wt %) at the room temperature. The film was then heated to 150 °C in the presence of benzoic acid, and a clear solution formed. The solution is then supercooled by placing the glass slide on a hot bar at 110 °C and contacting the edge of the coverslip with tweezers to induce crystallization of the BA ( $T_m^{BA} \cong 123$  °C). Rapid directional crystallization of the BA occurs, resulting in platelike crystals, whose sizes are about  $500 \times 200$   $\mu\text{m}$ , elongated in the crystallographic  $b$  direction, with large top and bottom (001) surfaces.<sup>38</sup> The slide is then moved to a position on the hot bar with a temperature of 60 °C and held for a minute to complete the crystallization of the BA and induce the crystallization of the PE component in the directionally solidified structure of the mixture of BA and the block copolymer and finally cooled to room temperature. The BA crystals were then dissolved in ethyl alcohol at 50 °C. The polymer film supported by the carbon film was floated off the glass onto water and picked up with copper grids (200 mesh) and analyzed in the transmission electron microscope in bright field and dark field mode as well as in selected area diffraction. Thin films of the copolymer crystallized by simple casting at room temperature from a xylene solution (0.1–0.3 wt %) on microscope glass slides were also analyzed for comparison. A JEOL 200CX and Philips CM12 TEM, operating at 200 and 120 kV, were used.

## Results and Discussion

Bulk samples of the PE/PEP/PE block copolymer were analyzed by simultaneous WAXS and SAXS in order to check whether the crystallization of the PE blocks occurs from a homogeneous melt or from an already microphase-separated heterogeneous state. Thin films were analyzed by electron diffraction and electron microscopy under both bright and dark field mode in order to observe the orientation of the PE crystals and the microdomain morphology which develop in the epitaxial crystallization process.

**Bulk Samples.** SAXS and WAXS patterns of the PE/PEP/PE bulk sample, recorded simultaneously at a series of temperatures, starting from the melt and cooling to room temperature, are shown in Figure 1, a and b, respectively. It is apparent that the SAXS pattern at 120 °C is essentially featureless, indicating that no microdomain structure is present in the melt. The correlation hole peak normally found in the disordered state of block copolymers is absent because of the very low electron density contrast between the PE and PEP blocks.<sup>16</sup> This is contrary to the higher molecular weight sample analyzed by Seguela and Prud'homme,<sup>8</sup> which yielded a microphase-separated melt. In our sample, the PE and PEP blocks are miscible in the melt (120 °C), which appears therefore as a homogeneous phase. The WAXS pattern of the melt (Figure 1b) at 120 °C presents a typical amorphous halo. The intensity of the amorphous halo decreases due to the crystallization of PE block (at 70 and 50 °C). The two crystalline peaks correspond to the {110} and {200} reflections of the usual orthorhombic form of PE.<sup>44</sup> In good correspondence to the temperature at which the crystalline peaks develop in the WAXS pattern, a peak at  $q = 0.16$   $\text{nm}^{-1}$ , corresponding to a Bragg distance of 40 nm, develops in the SAXS patterns, indicating the formation of a microphase-separated microstructure. The weak broad

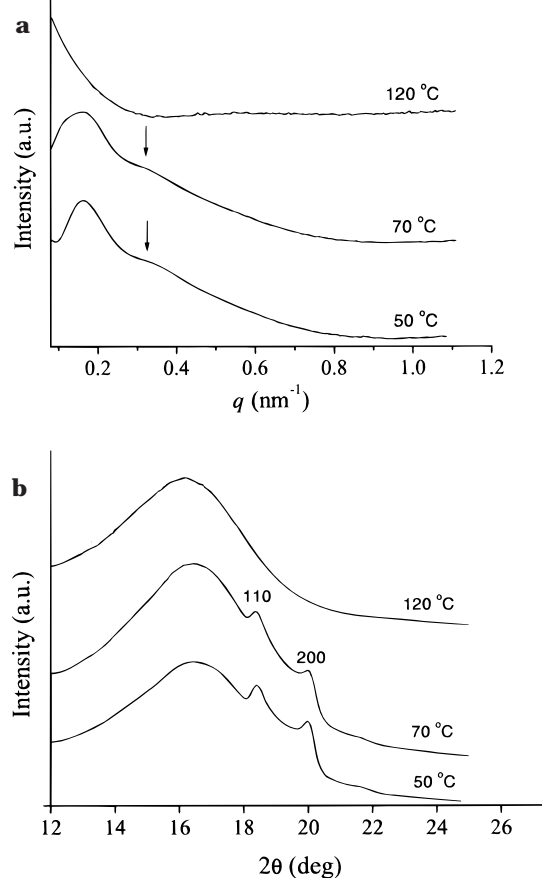


**Figure 1.** (a) Small-angle X-ray diffraction patterns and (b) wide-angle X-ray diffraction patterns of a bulk sample of the PE/PEP/PE block copolymer recorded at the indicated temperatures during cooling from a homogeneous melt.

reflection around  $0.32$   $\text{nm}^{-1}$ , indicated by arrows in Figure 1a, gives a ratio  $q_2/q_1$  of about 2, characteristic of a lamellar structure, as was previously found in the weak segregated semicrystalline block copolymers.<sup>13,16</sup> The parallel growth of the WAXS and SAXS peaks in the cooling step indicates that, in this sample of PE/PEP/PE block copolymer, the microphase separation is driven by crystallization from a single phase melt.

**Thin Films.** A bright-field TEM image of a thin film of the PE/PEP/PE sample, prepared by casting at room temperature on a microscope glass slide from dilute xylene solution, is shown in Figure 2. The PE blocks crystallize by evaporation of the solvent, and in Figure 2 radially oriented lamellar PE microdomains comprise volume-filling crystalline spherulites having an average diameter of 5–10  $\mu\text{m}$ .

To avoid the typical spherulite structure and control the morphology, thin films of the block copolymer were epitaxially crystallized onto the (001) surface of crystals of BA following the method outlined in the Experimental Section. The selected area electron diffraction pattern of the PE/PEP/PE block copolymer using a 6  $\mu\text{m}$  diameter SAD aperture is shown in Figure 3. The pattern essentially presents only the  $0kl$  reflections of PE; therefore, it corresponds to the  $b^*c^*$  section of the reciprocal lattice of PE. This indicates that a high orientation (single-crystal-like) of the chain molecules in the crystalline phase has been achieved. Since the  $b^*c^*$  section of the reciprocal lattice is in the diffraction condition, the chain axis of the crystalline PE lies flat on the substrate surface and oriented parallel to the  $a$  axis of BA crystals, as in the case of the PE homopoly-



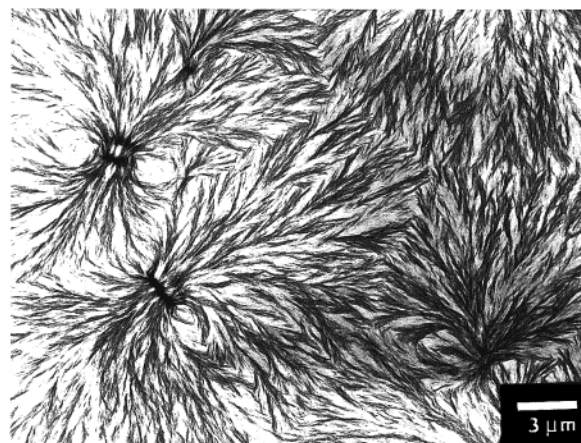


**Figure 2.** TEM bright-field image of a thin film of PE/PEP/PE block copolymer obtained by casting from a xylene solution. Radially oriented lamellar PE microdomains, characterized by crystalline spherulites having size of 5–10  $\mu\text{m}$ , are imaged through the diffraction contrast.

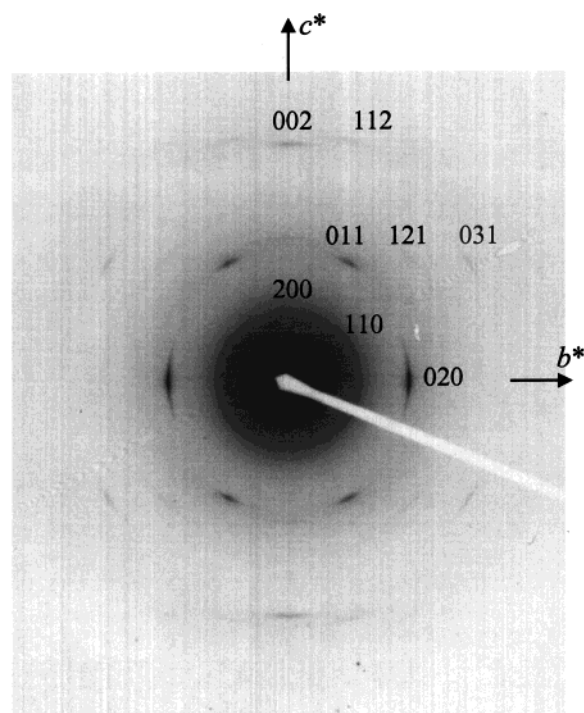
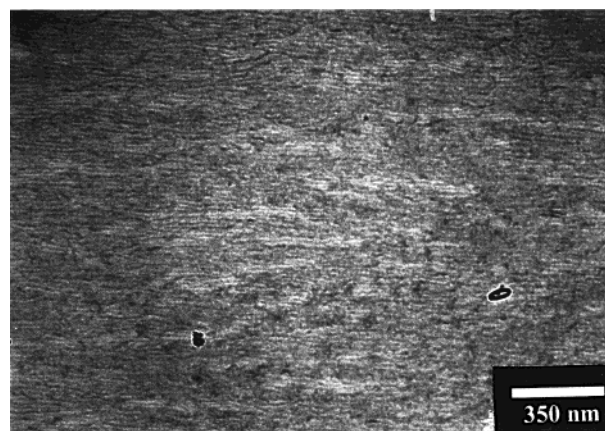
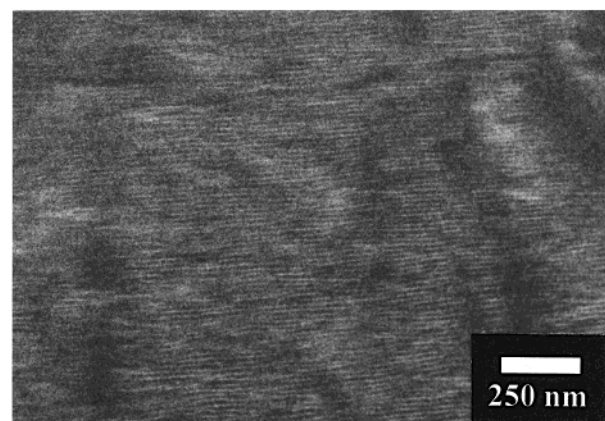


**Figure 3.** Selected area electron diffraction pattern of a thin film of PE/PEP/PE block copolymer epitaxially crystallized onto BA. The pattern presents mainly the  $0kl$  reflections of PE; hence, it indicates that the (100) plane of PE is normal to the electron beam and parallel to the (001) exposed face of the BA crystals. A small tilting of the lamellae around the  $b$  axis, or progressive tilting of successive stacks of lamellae, accounts for the presence of arced reflections as well as the  $1kl$  and  $2kl$  type reflections (in particular, 121 and 112 reflections) and the weak 110 and 200 reflections.

mer.<sup>38</sup> The (100) plane of PE is in contact with the (001) plane of BA;<sup>38</sup> therefore, the crystalline PE lamellae stand edge-on on the substrate surface, with PE  $b$  axis oriented parallel to the  $b$  axis of BA.<sup>38</sup> The relative orientation of PE and substrate lattices is therefore identical to that obtained for the polyethylene homopolymer.<sup>38</sup> The  $b$  and  $c$  axes of PE are parallel to the  $b$  and  $a$  axes of BA, respectively; this epitaxy is well explained in terms of matching the PE interchain distance of the  $b$  PE axis periodicity (4.95 Å) with the  $b$  periodicity of the BA unit cell (5.25 Å).<sup>37</sup>



(a)



(b)

**Figure 4.** (a) Under-focused TEM bright-field image of a thin film of PE/PEP/PE block copolymer epitaxially crystallized onto BA corresponding to an area similar to that of Figure 3. The light noncrystalline regions appear bright due to phase contrast.<sup>51</sup> The dark regions correspond to the denser crystalline PE phase, which form long lamellae standing edge-on on the substrate surface. The lamellae are preferentially oriented with the  $b$  axis of PE parallel to the  $b$  axis of the BA. (b) TEM (110) dark-field image of a thin film of PE/PEP/PE block copolymer epitaxially crystallized onto BA corresponding to an area similar to that of Figure 3. Long thin, highly parallel alternating regions of bright/dark contrast are evident over the field of view. The bright regions correspond to the crystalline PE lamellae in the Bragg condition. Dark regions crossing the lamellar structure correspond to crystalline areas where the crystals are tilted or twisted out of the Bragg condition.

A bright field TEM image of the film epitaxially crystallized onto BA is shown in Figure 4a. Phase contrast obtained by underfocus of the objective lens makes the noncrystalline regions appear bright.<sup>51</sup> Instead of a spherulitic structure, the epitaxy has produced a highly aligned lamellar structure with long, thin crystalline PE lamellae, with a thickness of 10–15 nm, oriented along the  $[010]_{\text{PE}}||[010]_{\text{BA}}$  direction. The average distance between the lamellae is 30–40 nm, in agreement with the bulk SAXS data, and the order extends over a larger than 100  $\mu\text{m}^2$  region.

Further details of the structure and orientation of the film can be made by dark field (DF) imaging of the PE crystalline lamellae. Since the film has a single-crystal-like orientation, dark field imaging using a single diffraction spot should reveal the entire set of crystalline regions. In view of the limited lifetime of PE crystals under the electron beam, it is preferable to use the

strongest 110 reflection to record DF images.<sup>45</sup> For this purpose, the epitaxially crystallized film was tilted by 34° about the  $c$  axis of PE in order to bring the 110 reflection in diffracting position. The corresponding DF image shown in Figure 4b reveals the same parallel array of crystalline PE lamellae, oriented along the  $b$  axis of BA crystals, with 40–50 nm interlamella spacing. The dark areas in the image correspond to regions slightly out of the Bragg condition due to a small amount of tilting.

The thickness of the crystalline PE domains is approximately 10–15 nm, almost comparable to that of amorphous PE and PEP layer. On the basis of the PE volume fraction, bulk crystallinity (30%), and microdomain lamellar repeat, a crystal thickness of around 4–5 nm would be expected for bulk crystallized material. The larger crystal thickness observed may be due to an enhancement of crystallinity by the substrate.<sup>46</sup>

In a recent paper,<sup>47</sup> we show that in strongly segregated semicrystalline block copolymers, epitaxially crystallized onto an organic substrate, the resulting structure can be understood in terms of a combination of directional solidification of the eutectic solution of the block copolymer in the crystallizable organic solvent and the following epitaxial crystallization of the crystalline block onto the organic crystalline substrate.<sup>47</sup> The eutectic behavior of binary solutions of a semicrystalline homopolymer and a crystallizable organic solvent has been described in the literature.<sup>48–50</sup> In the present case, where the two blocks are miscible above the crystallization temperature of the PE block (melt compatible semicrystalline block copolymer), the orientation of the microdomains occurs only due to epitaxial relationship of the PE block with the BA.

## Conclusions

We show how to control the microstructure of a semicrystalline block copolymer by a highly specific molecular interaction with the substrate. High orientation of the crystals and microdomains of a PE/PEP/PE triblock copolymer has been achieved through epitaxial crystallization of the copolymer, from the homogeneous melt, onto benzoic acid substrate crystals. The epitaxial crystallization is used to control the crystallization and the morphology of a thin film of block copolymer. Since the microphase separation is driven by crystallization from a homogeneous melt, the long-range orientation of the crystalline unit cell induces excellent alignment of the microdomains, as shown in the schematic model of Figure 5. The PE microdomains consist of long crystalline lamellae aligned parallel to a preferential crystallographic direction of the substrate (the  $b$  axis of the benzoic acid crystals, parallel to the  $b$  axis of PE). The combination of electron diffraction and bright and dark field images allows clear determination of the molecular chain orientation of PE with respect to the suprastructure of crystalline PE lamellae and PEP layers. The orientation of the PE unit cell, induced by the epitaxial relationship with the crystalline lattice of the substrate, is such that the PE molecular chain axis ( $\hat{c}$ ) is parallel to the normal direction ( $\hat{n}$ ) of lamellar plane, as shown in Figure 5. This result is in agreement with the model proposed by Rangarajan et al.<sup>13,16</sup> for semicrystalline block copolymer crystallized from the homogeneous melt. Our result is a consequence of the interaction with the substrate surface in the thin film and yields a globally oriented single-crystal-like texture of vertically oriented PE/PEP lamellae.

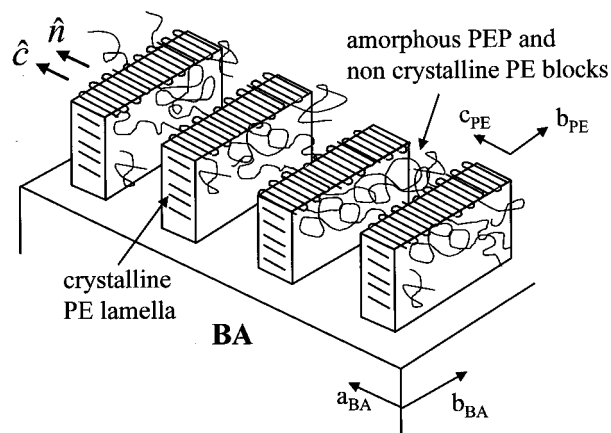


**Figure 5.** Schematic model showing the crystalline and amorphous microdomains in the PE/PEP/PE block copolymer epitaxially crystallized onto BA. Epitaxial relationship shows the relative orientation of the polyethylene lamellae on the benzoic acid.  $(100)_{PE} || (001)_{BA}$ , and  $c_{PE} || a_{BA}$ ,  $b_{PE} || b_{BA}$ . The orientation of the PE molecular chains perpendicular to the lamellar plane  $\hat{c} || \hat{n}$  is also shown.

**Acknowledgment.** This research was supported by National Science Foundation DMR98-07591, ACS-PRF, and US–France NSF-CNRS (INT9726544). We gratefully acknowledge Prof. B. S. Hsiao and Dr. F. Yeh for their help at the beamline X27C in BNL. We thank the MIT Center for Materials Science and Engineering for the use of the TEM facility and NSLS for the scattering facility. C. De Rosa thanks the University of Naples “Fedrico II” for the financial support of the short mobility research.

## References and Notes

- (1) Fredrickson, G. H.; Bates, F. S. *Annu. Rev. Phys. Chem.* **1990**, *41*, 525.
- (2) Leibler, L. *Macromolecules* **1980**, *13*, 1602.
- (3) Fredrickson, G. H.; Helfand, E. *J. Chem. Phys.* **1987**, *87*, 697.
- (4) Bates, F. S.; Bair, H. E.; Hartney, M. A. *Macromolecules* **1984**, *17*, 1987.
- (5) Skoulios, A. E.; Tsouladze, G.; Franta, E. *J. Polym. Sci.* **1963**, *C4*, 507.
- (6) Lotz, B.; Kovacs, A. J. *Kolloid Z.* **1966**, *209* (2), 97.
- (7) Lotz, B.; Kovacs, A. J.; Bassett, G. A.; Keller, A. *Kolloid Z.* **1966**, *209* (2), 115.
- (8) Seguela, R.; Prud'homme, J. *Polymer* **1989**, *30*, 1446.
- (9) Cohen, R. E.; Cheng, P. L.; Douzinas, K.; Kofinas, P.; Berney, C. V. *Macromolecules* **1990**, *23*, 324.
- (10) Douzinas, K. C.; Cohen, R. E.; Halasa, A. F. *Macromolecules* **1991**, *24*, 4457.
- (11) Douzinas, K. C.; Cohen, R. E. *Macromolecules* **1992**, *25*, 5030.
- (12) Nojima, S.; Kato, K.; Yamamoto, S.; Ashida, T. *Macromolecules* **1992**, *25*, 2237.
- (13) Rangarajan, P.; Register, R. A.; Fetters, L. J. *Macromolecules* **1993**, *26*, 4640.
- (14) Cohen, R. E.; Bellare, A.; Drzewinski, M. A. *Macromolecules* **1994**, *27*, 2321.
- (15) Kofinas, P.; Cohen, R. E. *Macromolecules* **1994**, *27*, 3002.
- (16) Rangarajan, P.; Register, R. A.; Adamson, D. H.; Fetters, L. J.; Bras, W.; Naylor, S.; Ryan, A. J. *Macromolecules* **1995**, *28*, 1428.
- (17) Rangarajan, P.; Register, R. A.; Fetters, L. J.; Bras, W.; Naylor, S.; Ryan, A. J. *Macromolecules* **1995**, *28*, 4932.
- (18) Ryan, A. J.; Hamley, I. W.; Bras, W.; Bates, F. S. *Macromolecules* **1995**, *28*, 3860.
- (19) Yang, Y.-W.; Tanodekaew, S.; Mai, S.-M.; Booth, C.; Ryan, A. J.; Bras, W.; Viras, K. *Macromolecules* **1995**, *28*, 6029.
- (20) Khandpur, A. K.; Macosko, C. W.; Bates, F. S. *J. Polym. Sci., Polym. Phys. Ed.* **1995**, *33*, 247.
- (21) Hamley, I. W.; Fairclough, J. P. A.; Terril, N. J.; Ryan, A. J.; Lipic, P. M.; Bates, F. S.; Town-Andrews, E. *Macromolecules* **1996**, *29*, 8835.
- (22) Hamley, I. W.; Fairclough, J. P. A.; Ryan, A. J.; Bates, F. S.; Town-Andrews, E. *Polymer* **1996**, *37*, 4425.



- (23) Ryan, A. J.; Fairclough, J. P. A.; Hamley, I. W.; Mai, S.-M.; Booth, C. *Macromolecules* **1997**, *30*, 1723.
- (24) Mai, S.-M.; Fairclough, J. P. A.; Viras, K.; Gorry, P. A.; Hamley, I. W.; Ryan, A. J.; Booth, C. *Macromolecules* **1997**, *30*, 8392.
- (25) Rangarajan, P.; Haisch, C. F.; Register, R. A.; Adamson, D. H.; Fetters, L. J. *Macromolecules* **1997**, *30*, 494.
- (26) Quiram, D. J.; Register, R. A.; Marchand, G. R. *Macromolecules* **1997**, *30*, 4551.
- (27) Quiram, D. J.; Register, R. A.; Marchand, G. R.; Ryan, A. J. *Macromolecules* **1997**, *30*, 8338.
- (28) Quiram, D. J.; Register, R. A.; Marchand, G. R.; Adamson, D. H. *Macromolecules* **1998**, *31*, 4891.
- (29) Hillmyer, M. A.; Bates, F. S. *Macromol. Symp.* **1997**, *117*, 121.
- (30) Balsamo, V.; von Gyldenfeldt, F.; Stadler, R. *Macromol. Chem. Phys.* **1996**, *197*, 3317.
- (31) Park, C.; Simmons, S.; Fetters, L. J.; Hsiao, B.; Yeh, F.; Thomas, E. L. *Polymer* **2000**, *41*, 2971.
- (32) Park, C.; De Rosa, C.; Fetters, L. J.; Thomas, E. L., to be submitted to *Macromolecules*.
- (33) Zhu, L.; Cheng, S. Z. D.; Calhoun, B. H.; Ge, Q.; Quirk, R. P.; Thomas, E. L.; Hsiao, B. S.; Yeh, F. *J. Am. Chem. Soc.*, accepted.
- (34) Di Marzo, E. A.; Guttman, C. M.; Hoffman, J. D. *Macromolecules* **1980**, *13*, 1194.
- (35) Whitmore, M. D.; Noolandi, J. *Macromolecules* **1988**, *21*, 1482.
- (36) Willems, J.; Willems, L. *Experientia* **1957**, *13*, 465. Willems, J. *Discuss. Faraday Soc.* **1958**, *25*, 111. Fischer, E. H. *Discuss. Faraday Soc.* **1958**, *25*, 204. Fischer, E. W. *Kolloid Z.* **1958**, *169*, 108. Wellingshoff, S. H.; Rybnikar, F.; Baer, E. *J. Macromol. Sci., Phys.* **1974**, *B10*, 1.
- (37) Wittmann, J. C.; Smith, P. *Nature* **1991**, *352*, 414.
- (38) Wittmann, J. C.; Hodge, A. M.; Lotz, B. *J. Polym. Sci., Polym. Phys. Ed.* **1983**, *21*, 2495.
- (39) Wittmann, J. C.; Lotz, B. *J. Polym. Sci., Polym. Phys. Ed.* **1981**, *19*, 1837.
- (40) Morton, M.; Fetters, L. J. *Rubber Chem. Technol.* **1975**, *48*, 359.
- (41) Rachapudy, H.; Smith, G. G.; Rayn, V. R.; Graessley, W. W. *J. Polym. Sci., Polym. Phys. Ed.* **1979**, *17*, 1211.
- (42) Xu, Z.; Hadjichristidis, N.; Fetters, L. J.; Mays, J. W. *Adv. Polym. Sci.* **1995**, *120*, 1.
- (43) Wunderlich, B. *Macromolecular Physics*; Academic Press: New York, 1973; Vol. 1, Chapter 4.
- (44) Bunn, C. W. *Trans. Faraday Soc.* **1939**, *35*, 482.
- (45) Thomas, E. L.; Ast, D. *Polymer* **1974**, *15*, 37.
- (46) Wu, S. *Polymer Interface and Adhesion*; Marcel Dekker: New York, 1982; Chapter 5.
- (47) De Rosa, C.; Park, C.; Thomas, E. L.; Lotz, B. *Nature* **2000**, *405*, 433.
- (48) Smith, P.; Pennings, A. J. *Polymer* **1974**, *15*, 413.
- (49) Wittmann, J. C.; John Manley, R. St. *J. Polym. Sci., Polym. Phys. Ed.* **1977**, *15*, 1089.
- (50) Hodge, A. M.; Kiss, G.; Lotz, B.; Wittmann, J. C. *Polymer* **1982**, *23*, 985.
- (51) Petermann, J.; Gohil, R. M. *J. Mater. Sci.* **1979**, *14*, 2260.

MA992132M